$$HCOONH_4 \rightarrow HCONH_2 + H_2O \quad (7)$$

$$CrO_3 + H_2O \rightarrow 2H^+ + CrO_4^{2-} \quad (8)$$

into $HCONH_2$ and H_2O was reported by Suzuki et al.;[1] i.e., the decomposition amount of $HCOONH_4$ is equivalent to that of CrO_3. As the CrO_4^{2-} anions are stable, it was concluded that there exist mononuclear CrO_4^{2-} tetrahedra with Cr–O bond lengths of 1.61 Å at the initial state of the dissolution of CrO_3 in the $HCONH_2$ + $HCOONH_4$ solvent.

Next, $HCOONH_4$ dissociates into the $HCOO^-$ and NH_4^+ ions in a solvent with a large dielectric constant, such as $HCONH_2$ (109 at 20 °C). The NH_4^+ ion decomposes into H^+ and NH_3, and NH_3 leaves the system at 90 °C (eq 9). When the tem-

$$HCOONH_4 \rightarrow HCOO^- + H^+ + NH_3\uparrow \quad (9)$$

perature of the system is increased, Cr(VI) ions are reduced by the heated $HCOO^-$ anions, as shown in eq 10–12. Thus, Cr(III)

$$HCOO^- \rightarrow {}^1/_2H_2\uparrow + CO_2\uparrow + e^- \quad (10)$$

$$CrO_4^{2-} + 3e^- \rightarrow Cr^{3+} + 4O^{2-} \quad (11)$$

$$O^{2-} + 2H^+ \rightarrow H_2O\uparrow \quad (12)$$

ions are coordinated to six O atoms with high electron densities coming from either $HCOO^-$ ions or $HCONH_2$ molecules and form octahedral complexes in solution II as shown in eq 13, where x

$$Cr^{3+} + xHCOO^- + yHCONH_2 \rightarrow [Cr(HCOO)_x(HCONH_2)_y]^{3-x} \quad (13)$$

+ $y = 6$. The Cr ions were considered not to be coordinated to N atoms because, in addition to the reason mentioned above, the Cu ions, which form amine complexes more easily than the Cr ions, were found to be bonded to the O atoms in the $HCONH_2$ + $HCOONH_4$ system by ESR spectral analyses.[1] The formation of anionic complexes of Cr(III) ions in solution II was supported by the experimental results that Cr(III) ions were removed by OH^-form anion-exchange resin;[27] i.e., removal ratios by OH^- and H^+ resins are 95 and 3%, respectively. Only one of two O atoms in the $HCOO^-$ ion is shared at the corner of the octahedron because the O···O distance within the octahedron is about 2.83 Å and that within the $HCOO^-$ ion is about 2.22 Å. Therefore, x was considered to be equal to 4, 5, or 6 although it is difficult to decide the exact value of x. From the above examination, the mononuclear $[Cr(HCOO)_x(HCONH_2)_y]^{3-x}$ ($x + y = 6$; $4 \leq x \leq 6$) octahedra with Cr–O bond lengths of 2.00 Å were concluded to be produced in the $HCONH_2$ + $HCOONH_4$ system by heating reduction. The blackish corrosion-resistant chromium film produced by electrodeposition[2] is probably ascribed to the existence of $[Cr(HCOO)_x(HCONH_2)_y]^{3-x}$ complexes in the $HCONH_2$ + $HCOONH_4$ system.

Acknowledgment. This work was supported by a Grant-in-Aid for Encouragement of Research A from the Japanese Ministry of Education (No. 58750633). We thank the staff of the Photon Factory of the National Laboratory for High Energy Physics (KEK) for providing beam time. The computations were carried out on an ACOS 850 computer at the Computer Center of Yamanashi University.

Registry No. CrO_4^{2-}, 13907-45-4; CrO_3, 1333-82-0; $HCOONH_4$, 540-69-2; $HCONH_2$, 75-12-7.

(27) Ayuzawa, N.; Hayakawa, Y.; Suzuki, T. *Denki Kagaku oyobi Kogyo Butsuri Kagaku* **1981**, *49*, 521.

Notes

Contribution from the Departments of Chemistry, University of Hong Kong, Hong Kong, and The Chinese University of Hong Kong, Shatin, New Territories, Hong Kong

High-Valent Schiff-Base Complexes of Osmium. X-ray Crystal Structure of *trans*-[Os^{IV}(salen)$(SPh)_2$]

Chi-Ming Che,*[1a] Wing-Kin Cheng,[1a] and Thomas C. W. Mak*[1b]

Received March 26, 1985

High-valent iron, ruthenium, and osmium metalloporphyrin complexes containing oxide (O^{2-}), alkoxide (OR^-), or mercaptide (SR^-) ligands are potentially useful model systems for cytochromes or oxygenase. As part of a program to investigate the chemistry of osmoglobin,[2] we have been interested in the chemistry of osmium Schiff-base complexes because these species are expected to exhibit chemistry similar to that of the analogous porphyrin.[3] Here the synthesis and characterization of some high-valent Schiff-base complexes of osmium are described.

Experimental Section

Materials. $K_2[OsO_2(OH)_4]$ and $salenH_2$ (salen = *N*,*N*′-ethylenebis(salicyclideneaminate)) were prepared as described in the literature.[4] All solvents used were of analytical grade. Triphenylphosphine (Merck 98%) and thiophenol (Aldrich 99%) were used as supplied.

***trans*-[Os^{VI}(salen)O_2] (1).** $K_2[OsO_2(OH)_4]$ (0.5 g) and $salenH_2$ (0.4 g) were stirred in methanol (150 mL) for 30 min. An orange-red solid gradually formed. This is filtered off, washed with a methanol/diethyl ether mixture (1:10), and dried under vacuum at room temperature; yield 85%. Anal. Calcd for $OsC_{16}H_{14}N_2O_4$: C, 39.34; H, 2.86; N, 5.75. Found: C, 39.43; H, 2.62; N, 5.84. IR ν(Os=O): 840 cm^{-1}. The complex is virtually insoluble in common organic solvents.

***trans*-[Os^{IV}(salen)$(OMe)_2$] (2a).** A methanolic suspension of **1** (0.5 g in 100 mL) and PPh_3 (1.4 g) was heated with stirring at 50 °C for 20 min. A deep red-brown solution was obtained, which was then filtered off and rotatory evaporated to dryness. The dry residue was dissoved in CH_2Cl_2 and transferred to the top of a silica gel column. The PPh_3 was removed by eluting with CH_2Cl_2 (300 mL), and the Os(IV) product was eluted out as a brick red band by using acetone/methanol (1:1) mixture as the eluent. Crystals of **2a** were obtained by slow diffusion of hexane into a dichloromethane solution of the crude product. Yield: ~75%. Anal. Calcd for $OsC_{18}H_{20}N_2O_4$: C, 41.68; H, 3.86; N, 5.40. Found: C, 41.2; H, 3.85; N, 5.25. UV–vis spectrum in CH_3CN, λ_{max}/nm (ϵ_{max}/(dm^3 mol^{-1} cm^{-1})): 413 (10 500), 352 (11 900), 252 (8200).

***trans*-[Os^{IV}(salen)$(OEt)_2$] (2b).** The complex was similarly prepared as described for **2a** except that absolute ethanol was used instead of methanol. Yield: ~68%. Anal. Calcd for $OsC_{20}H_{24}N_2O_4$: C, 43.96; H, 4.39; N, 5.13. Found: C, 43.70; H, 4.10; N, 4.95. UV–vis spectrum in CH_3CN, λ_{max}/nm (ϵ_{max}/(dm^3 cm^{-1} mol^{-1})): 410 (17 700), 350 (15 500), 255 (15 100).

***trans*-[Os^{IV}(salen)$(SPh)_2$] (3).** Thiophenol (5 mL) was added dropwise to a stirred dichloromethane suspension of **1** (0.5 g in 100 mL). After 15 min, a deep bluish green solution was obtained. This was evaporated off to dryness. The crude solid was washed with petroleum ether (60–80 °C) to remove excess thiophenol and purified on a silica gel column with CH_2Cl_2 as the eluent. Blue crystalline solids of **3** were

(1) (a) University of Hong Kong. (b) The Chinese University of Hong Kong.
(2) Margalit, R.; Pecht, I.; Che, C.-M.; Chiang, H.-J.; Gray, H. B., "Abstracts of Papers" 185th National Meeting of the American Chemical Society, Seattle, WA, March 22, 1983; American Chemical Society: Washington, DC; INOR 42.
(3) Che, C.-M.; Poon, C. K.; Chung, W. C.; Gray, H. B. *Inorg. Chem.* **1985**, *24*, 1277.
(4) (a) Malin, J. M. *Inorg. Synth.* **1980**, *20*, 61. (b) Earnshaw, A.; King, E. A.; Larkworthy, L. F. *J. Chem. Soc. A* **1968**, 1048.

0020-1669/86/1325-0703$01.50/0

Table I. Atomic Coordinates (×10⁵ for Os; ×10⁴ for Other Atoms) and Thermal Parameters (×10⁴ for Os; ×10³ for Other Atoms)

atom	x	y	z	U_{eq}, Å²
Os	17228 (3)	7535 (2)	24776 (3)	422 (1)[a]
S(1)	961 (2)	590 (2)	4212 (2)	53 (1)[a]
S(2)	2277 (2)	1039 (2)	655 (2)	61 (1)[a]
O(1)	3097 (5)	1306 (4)	3252 (5)	53 (2)[a]
O(2)	2717 (5)	−125 (4)	2609 (5)	51 (2)[a]
N(1)	656 (6)	1599 (4)	2269 (6)	49 (3)[a]
N(2)	278 (6)	261 (5)	1770 (6)	53 (3)[a]
C(1)	−456 (8)	1464 (6)	1556 (11)	80 (5)[a]
C(2)	918 (8)	2226 (6)	2621 (8)	57 (3)[a]
C(3)	1997 (8)	2420 (5)	3287 (8)	57 (3)[a]
C(4)	2995 (8)	1966 (5)	3614 (7)	53 (3)[a]
C(5)	3931 (9)	2229 (6)	4346 (8)	63 (4)[a]
C(6)	3963 (10)	2915 (7)	4716 (9)	79 (5)[a]
C(7)	3043 (11)	3375 (8)	4377 (11)	94 (6)[a]
C(8)	2088 (11)	3131 (6)	3692 (9)	73 (4)[a]
C(9)	−793 (9)	710 (6)	1578 (11)	77 (4)[a]
C(10)	186 (8)	−423 (6)	1643 (8)	56 (3)[a]
C(11)	1089 (9)	−933 (5)	1986 (8)	56 (3)[a]
C(12)	2272 (9)	−766 (5)	2461 (7)	52 (3)[a]
C(13)	3020 (9)	−1342 (6)	2828 (8)	62 (4)[a]
C(14)	2636 (11)	−2021 (6)	2750 (10)	80 (5)[a]
C(15)	1473 (13)	−2191 (6)	2302 (11)	94 (6)[a]
C(16)	727 (11)	−1659 (7)	1933 (9)	75 (5)[a]
C(17)	1780 (4)	906 (3)	6365 (5)	56 (2)
C(18)	2614 (4)	931 (3)	7312 (5)	64 (3)
C(19)	3743 (4)	636 (3)	7251 (5)	63 (3)
C(20)	4036 (4)	316 (3)	6241 (5)	70 (3)
C(21)	3202 (4)	291 (3)	5293 (5)	62 (3)
C(22)	2074 (4)	586 (3)	5354 (5)	49 (2)
C(23)	4191 (5)	1780 (3)	65 (6)	66 (3)
C(24)	5398 (5)	1885 (3)	−64 (6)	72 (3)
C(25)	6239 (5)	1399 (3)	398 (6)	76 (3)
C(26)	5874 (5)	808 (3)	988 (6)	114 (5)
C(27)	4667 (5)	703 (3)	1117 (6)	104 (5)
C(28)	3826 (5)	1188 (3)	656 (6)	54 (2)

[a] Equivalent isotropic temperature factor U_{eq} calculated as one-third of the trace of the orthogonalized U_{ij} matrix.

obtained by slow diffusion of hexane into a dichloromethane solution of the crude product. Yield: ~70%. Anal. Calcd. for $OsC_{28}H_{24}N_2S_2O_2$: C, 49.83; H, 3.59; N, 4.15. Found: C, 48.76; H, 3.33; N, 4.07. UV–vis spectrum in CH_3CN, λ_{max}/nm (ϵ_{max}/(dm³ mol⁻¹ cm⁻¹)): 705 (13 300), 625 (11 500), 400 (10 300), 353 (19 100).

Physical Measurements. Elemental analyses were performed by the Australian National Laboratory. IR spectra of Nujol mulls were measured on a Perkin-Elmer 577 spectrometer (4000–200 cm⁻¹). Electronic absorption spectra of freshly prepared solutions were measured with a Beckman Acta CIII spectrophotometer. ^1H NMR spectra were measured on a JEOL FX90Q Fourier transform NMR spectrometer, using tetramethylsilane as an internal reference.

X-ray Structural Determination of *trans*-[Os^{IV}(salen)(SPh)$_2$]. Crystal data for **3**: $OsC_{28}H_{24}N_2O_2S_2$, M_r = 674.84, space group $P2_1/a$, a = 11.265 (2) Å, b = 18.890 (6) Å, c = 11.740 (1) Å, β = 94.92 (1)°, V = 2489 (1) Å³, Z = 4, $F(000)$ = 1319.66, D_{measd} (flotation in CCl_4/$BrCH_2CH_2Br$) = 1.806, D_{calcd} = 1.801 g cm⁻³, μ(Mo Kα) = 53.19 cm⁻¹. Intensities ($h,k,\pm l$; 4622 unique data) were measured at 22 °C by using the ω–2θ variable scan (2.02–8.37° min⁻¹) technique in the bisecting mode up to $2\theta_{max}$ = 54°. Azimuthal scans of selected strong reflections over a range of 2θ values were used to define a pseudoellipsoid for the application of absorption correction (μr = 0.35, transmission factor = 0.248–0.359).[5,6] The structure was solved by the heavy-atom method. The two phenyl rings were treated as rigid groups, and the remaining non-hydrogen atoms were varied anisotropically. Hydrogen atoms were geometrically generated and assigned isotropic temperature factors. Convergence for 3788 (n) observed data ($|F_o| > 3\sigma|F_o|$) and 232 (p) variable data was reached at $R = \Delta/\sum|F_o|$ = 0.050 and $R_G = [\sum w\Delta^2/\sum w|F_o|^2]^{1/2}$ = 0.057, where $\Delta \equiv ||F_o| - |F_c||$ and $w = [\sigma^2(|F_o|) + 0.008|F_o|^2]^{-1}$. The goodness-of-fit index $S = [\sum w\Delta^2/(n-p)]^{1/2}$ has the value 1.287, and residual extrema in the final difference map lie between +1.2 and −1.65 e Å⁻³. Final positional and thermal parameters of non-hydrogen atoms are tabulated in Table I.

Bond distances, bond angles and selected torsion angles are listed in Table II. Tables of anisotropic temperature factors, atomic coordinates and thermal parameters for hydrogen atoms, and structure factors are available as supplementary material.

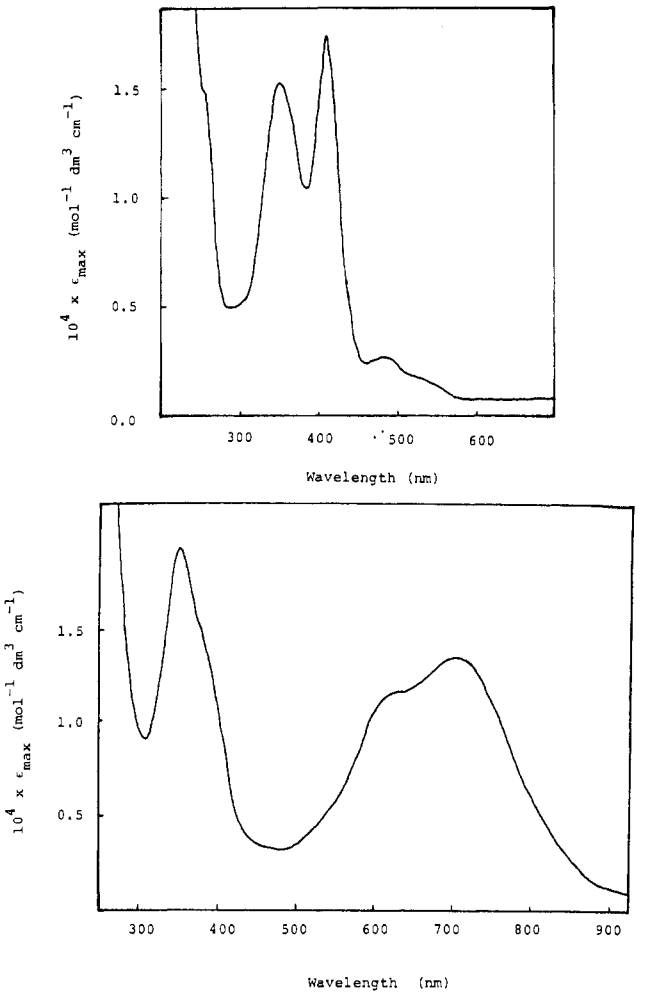

Figure 1. UV–vis spectra of acetonitrile solutions of (a) **2b** and (b) **3**.

Results and Discussion

As with the synthesis of other *trans*-Os$^{VI}O_2$ complexes containing multianionic chelating ligands,[7] $K_2[OsO_2(OH)_4]$ is a versatile starting material for the insertion of osmium into the salenH_2 ligand. Complex **1** is diamagnetic and exhibits an intense IR stretch at 840 cm⁻¹ characteristic of the ν_{as}(Os=O) stretch of *trans*-Os$^{VI}O_2$ complexes. Reduction of **1** with N_2H_4 in tetrahydrofuran yielded a diamagnetic dinitrogen complex [Os^{II}(salen)N_2(THF)] characterized by its IR absorption band at 2030 cm⁻¹ (νN≡N)). As in the case of [Os^{II}(OEP)N_2(THF)],[8] this species is unstable upon exposure to air. Reactions of **1** with PhSH or PPh_3 + ROH yielded Os(IV) complexes containing OR^- or SR^- as ligands. Complexes **2a**, **2b**, and **3** are air-stable diamagnetic crystalline solids; their IR spectral data in the 1700–1500-cm⁻¹ region are tabulated in Table III. In each case, the ν(O–H) stretch at 2600 cm⁻¹ of the salenH_2 is absent, indicating that the phenolic O–H groups are all deprotonated. Bands at 1600 and 1530 cm⁻¹ are assigned to ν(C=N) and ν(C—O), respectively. The electronic absorption spectra of the Os(IV) complexes (Figure 1) exhibit intense ligand-to-metal charge-transfer transition. The 705- and 625-nm bands in **3** are attributed to p_π(S) → d_π(Os(IV)) transitions; the observed red-shift from the p_π(OR) → d_π(Os(IV))

(5) Sparks, R. A. In "Crystallographic Computing Techniques"; Ahmad, F. R., Ed.; Munksgaard: Copenhagen, 1976; p 452.
(6) (a) Kopfmann, G.; Huber, R. *Acta Crystallogr., Sect. A: Cryst. Phys., Diffr., Theor. Gen. Crystallogr.* **1968**, *A24*, 348. (b) North, A. C. T.; Phillips, D. C.; Mathews, F. S. *Ibid.* **1968**, *A24*, 351.
(7) See for example: Christie, J. A.; Collins, T. J.; Kraft, T. E.; Santarsiero, B. D.; Spies, G. H. *J. Chem. Soc., Chem. Commun.* **1984**, 198.
(8) Buchler, J. W.; Smith, P. D. *Angew. Chem., Int. Ed. Engl.* **1974**, *13*, 745.

Table II. Bond Distances (Å), Bond Angles (deg) and Selected Torsion Angles (deg)

Os–S(1)	2.298 (2)	Os–S(2)	2.343 (2)	C(3)–C(4)	1.439 (13)	C(3)–C(8)	1.426 (16)
Os–O(1)	2.018 (6)	Os–O(2)	2.001 (6)	C(4)–C(5)	1.393 (13)	C(5)–C(6)	1.365 (17)
Os–N(1)	2.000 (8)	Os–N(2)	1.993 (7)	C(6)–C(7)	1.384 (18)	C(7)–C(8)	1.366 (17)
S(1)–C(22)	1.755 (6)	S(2)–C(28)	1.767 (6)	C(10)–C(11)	1.434 (14)	C(11)–C(12)	1.435 (13)
O(1)–C(4)	1.326 (12)	O(2)–C(12)	1.316 (12)	C(11)–C(16)	1.429 (16)	C(12)–C(13)	1.419 (14)
N(1)–C(1)	1.468 (12)	N(1)–C(2)	1.282 (14)	C(13)–C(14)	1.355 (16)	C(14)–C(15)	1.407 (19)
N(2)–C(9)	1.476 (13)	N(2)–C(10)	1.305 (15)	C(15)–C(16)	1.357 (18)		
C(1)–C(9)	1.474 (16)	C(2)–C(3)	1.435 (13)				
S(1)–Os–S(2)	171.7 (1)	S(1)–Os–O(1)	90.0 (2)	C(2)–C(3)–C(8)	117.1 (9)	C(4)–C(3)–C(8)	116.1 (9)
S(2)–Os–O(1)	92.2 (2)	S(1)–Os–O(2)	94.0 (2)	O(1)–C(4)–C(3)	124.2 (8)	O(1)–C(4)–C(5)	116.8 (8)
S(2)–Os–O(2)	94.0 (2)	O(1)–Os–O(2)	89.5 (3)	C(3)–C(4)–C(5)	119.0 (9)	C(4)–C(5)–C(6)	122.2 (10)
S(1)–Os–N(1)	87.1 (2)	S(2)–Os–N(1)	84.8 (2)	C(5)–C(6)–C(7)	120.3 (10)	C(6)–C(7)–C(8)	119.3 (12)
O(1)–Os–N(1)	94.1 (3)	O(2)–Os–N(1)	176.2 (3)	C(3)–C(8)–C(7)	122.9 (11)	N(2)–C(9)–C(1)	110.4 (8)
S(1)–Os–N(2)	87.3 (2)	S(2)–Os–N(2)	89.9 (2)	N(2)–C(10)–C(11)	125.9 (8)	C(10)–C(11)–C(12)	125.0 (9)
O(1)–Os–N(2)	175.4 (3)	O(2)–Os–N(2)	94.4 (3)	C(10)–C(11)–C(16)	116.0 (9)	C(12)–C(11)–C(16)	118.8 (9)
N(1)–Os–N(2)	82.0 (3)	Os–S(1)–C(22)	112.4 (2)	O(2)–C(12)–C(11)	125.8 (9)	O(2)–C(12)–C(13)	117.1 (8)
Os–S(2)–C(28)	112.1 (2)	Os–O(1)–C(4)	123.1 (5)	C(11)–C(12)–C(13)	117.2 (9)	C(12)–C(13)–C(14)	121.8 (10)
Os–O(2)–C(12)	123.3 (6)	Os–N(1)–C(1)	113.9 (7)	C(13)–C(14)–C(15)	121.5 (11)	C(14)–C(15)–C(16)	118.8 (11)
Os–N(1)–C(2)	125.4 (6)	C(1)–N(1)–C(2)	120.4 (8)	C(11)–C(16)–C(15)	122.0 (11)		
Os–N(2)–C(9)	115.1 (7)	Os–N(2)–C(10)	124.3 (6)	S(1)–C(22)–C(17)	116.2 (2)	S(1)–C(22)–C(21)	123.8 (2)
C(9)–N(2)–C(10)	119.7 (8)	N(1)–C(1)–C(9)	111.5 (9)	S(2)–C(28)–C(23)	117.4 (2)	S(2)–C(28)–C(27)	122.2 (2)
N(1)–C(2)–C(3)	124.9 (9)	C(2)–C(3)–C(4)	126.8 (9)				

N(1)–C(1)–C(9)–N(2)	−29.1 (13)		
Os–N(1)–C(1)–C(9)	25.4 (11)	Os–N(2)–C(9)–C(1)	20.8 (12)
N(2)–Os–N(1)–C(1)	−10.9 (7)	C(9)–N(2)–Os–N(1)	−5.7 (7)
Os–N(1)–C(2)–C(3)	−3.9 (13)	Os–N(2)–C(10)–C(11)	0.1 (13)
N(1)–C(2)–C(3)–C(4)	4.2 (16)	N(2)–C(10)–C(11)–C(12)	−4.1 (16)
C(2)–C(3)–C(4)–O(1)	6.2 (15)	C(10)–C(11)–C(12)–O(2)	−3.0 (15)
C(3)–C(4)–O(1)–Os	−14.4 (12)	C(11)–C(12)–O(2)–Os	12.4 (12)
C(4)–O(1)–Os–N(1)	11.5 (7)	C(12)–O(2)–Os–N(2)	−12.3 (7)
O(1)–Os–N(1)–C(2)	−2.6 (8)	O(2)–Os–N(2)–C(10)	6.4 (8)

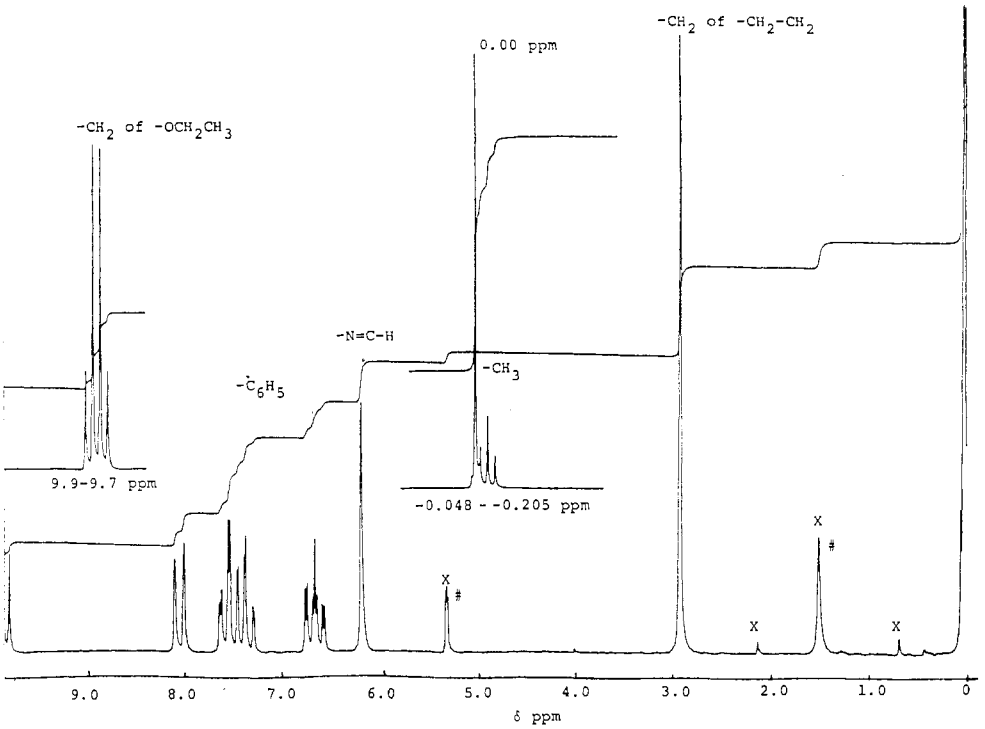

Figure 2. ^1H NMR spectrum of **2b** in CD_2Cl_2 with Me_4Si as internal reference.

bands in **2a** (415 nm) and **2b** (410 nm) is in accord with the charge-transfer nature of these transitions. The ^1H NMR spectra data of Os–salen complexes are tabulated in Table IV. Due to the poor solubility of **1** in most organic solvents, its ^1H NMR spectrum has not been recorded. As in free salenH_2 ligand, the bridging methylene protons are all equivalent and appear as a singlet at δ = 2.8–2.9. The observed downfield shift of the azomethine protons from **2a** (6.18 ppm) to **3** (12.0 ppm) is in accord with the larger shielding effect of the SC_6H_5 over the OMe group. The methylene and methyl protons of the coordinated OC_2H_5 group in **2b** are centered at δ = 9.8 (triplet) and −0.13 (quartet), respectively (Figure 2). As expected, the signal for the axial OCH_3 protons at δ = 8.95 (singlet) is similar to that of the methylene protons OCH_2CH_3 in **2b**.

A perspective view of **3** is shown in Figure 3. The structure constitutes the first reported example of a (thiolato)osmium(IV) complex. The coordination geometry of osmium is distorted octahedral, and both phenyl groups tilt away from the methylene bridge of the salen ligand, which is in the *gauche* conformation. The observed Os–O bond lengths (Os–O(1) = 2.018 (6) Å and Os–O(2) = 2.001 (6) Å) are typical of Os(IV)–O(phenoxide) bond distances found in a number of Os(IV)–(η^4-CHBA-Et) complexes,[9]

Table III. Infrared Spectra[a] of Osmium-salen Complexes in the 1650-1500-cm^{-1} Region

complexes	absorption bands, cm^{-1}
1	1630 (s), 1595 (s), 1525 (m)
2a	1605 (s), 1590 (s), 1530 (s)
2b	1600 (s), 1590((s), 1530 (s)
3	1600 (s), 1525 (s)

[a] All spectra were measured as Nujol mulls on KBr or NaCl plates. Abbreviations: s, strong; m, medium.

Table IV. ^{1}H NMR Spectral Data[a] for Os(IV)-salen Complexes

complexes	aromatic protons	azomethine protons	ethylene bridge protons	axial ligand protons
2a	6.60-8.10 (m)	6.24 (s)	2.86	8.95 (s)
2b	6.55-8.06 (m)	6.18(s)	2.90 (s)	9.8 (t), -0.13 (q)
3	5.78-8.26 (m)	12.0 (s)	2.80 (s)	*b*

[a] NMR spectra were recorded in CD_2Cl_2 solutions, and chemical shift (δ) values were reported from Me_4Si (δ = 0.0) as internal standard. The patterns of the signals were given in parentheses. Abbreviations: s, singlet; q, quartet; t, triplet; m, multiplet. [b] Obscured by aromatic protons of the chelate.

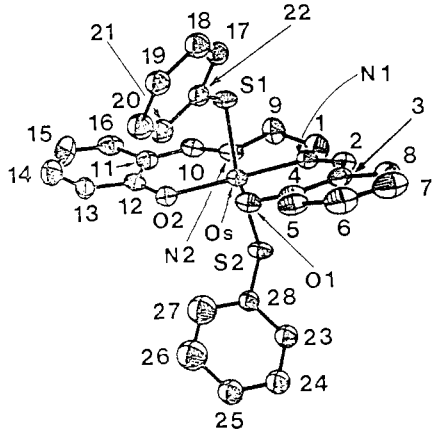

Figure 3. Persepctive view of **3**. Thermal ellipsoids are drawn at the 30% probability level.

where H_4-CHBA-Et stands for 1,2-bis(3,5-dichloro-2-hydroxybenzamido)ethene. The Os-S(1) and Os-S(2) bonds measure 2.298 (2) and 2.343 (2) Å, respectively, which are appreciably shorter than the Os(IV)-S bond distances (2.36-2.45 Å) in $[Os_2(Et_2dtc)_6][PF_6]_2$ (Et_2dtc = *N,N'*-diethyldithiocarbamato).[10] The Os-N bond distances (Os-N(1) = 2.000 (8) Å and Os-N(2) = 1.993 (7) Å) are normal, and bond lengths and angles for the salen ligand are in agreement with the mean values reported for a series of salen complexes.[11]

Acknowledgment. This research was supported by the Committee of Conference and Research Grants of the University of Hong Kong (C.-M.C and W.-K.C.). W.-K.C. acknowledges a graduate studentship from the Croucher Foundation.

Registry No. **1**, 99727-74-9; **2a**, 99748-39-7; **2b**, 99727-75-0; **3**, 99727-76-1; $K_2[OsO_2(OH)_4]$, 77347-87-6.

Supplementary Material Available: Tables of anisotropic temperature factors, atomic coordinates and thermal parameters of hydrogen atoms, and structure factors (25 pages). Ordering information is given on any current masthead page.

(9) See for example: Anson, F. C.; Christie, J. A.; Collins, T. J.; Coots, R. J.; Furutani, T. T.; Gipson, S. J.;Keech, J. T.; Kraft, T. E.; Santarsiero, B. D.; Spies, G. H. *J. Am. Chem. Soc.* **1984**, *106*, 4460.
(10) Wheeler, S. H.; Pignolet, L. H. *Inorg. Chem.* **1980**, *19*, 972.
(11) Calligaris, M.; Nardin, G.; Randascio, L. *Coord. Chem. Rev.* **1972**, *7*, 385.

Contribution from the Department of Chemistry, Columbia University in the City of New York, New York, New York 10027

Effects of Optical Density, Extinction Coefficient, and Window Area on Quantum Yields: Application to Mechanistic Problems in Organometallic Photochemistry

Alan S. Goldman and David R. Tyler*

Received March 7, 1985

We and others[1-3] have investigated the effects of light intensity on observed quantum yields. To the best of our knowledge, however, it has not been pointed out in the literature that parameters such as the extinction coefficient and window area can also have pronounced effects on the observed quantum yield. In particular, because the quantum yield can vary with the extinction coefficient, a change in the observed quantum yield corresponding to a change in wavelength may be due only to the different extinction coefficients at the respective wavelengths. In such a case, any conclusions regarding the photochemistry or photophysics drawn on the assumption of a true wavelength effect will be incorrect. In this note we quantify the effects that optical density, radiation intensity, and window area can have on the observed quantum yield, and we discuss the origin of these effects.

Results and Discussion

Although it is relatively simple to distribute heat homogeneously throughout a reaction solution, it is rare that a photoreaction solution will be "homogeneous in photons". As a result of both the Beer-Lambert law and the fact that radiation is typically not focused evenly over the entire surface of the reaction vessel, each point within the reaction mixture will experience a different photon flux. For an intramolecular reaction (e.g. olefin cis-trans isomerization) this phenomenon will not affect the quantum yield. However, when a reaction that is first order in a short-lived intermediate is in competition with a second-order reaction between two photoproduct species, the quantum yield will be affected by the *local* steady-state concentrations of these transient photoproducts and, therefore, by the amount of light absorbed at each point in the solution. The extent to which stirring can homogenize the solution depends upon the lifetimes of these species; it must be remembered that stirring can be slow on the time scale of many "fast" intermolecular reactions.

Reactions involving radicals are probably the most common type of reaction in which the quantum yield can be affected by the local steady-state concentrations of transient intermediates. As an example, consider the radical reaction in Scheme I in which a photogenerated metal radical abstracts a halogen atom from an alkyl halide.

Scheme I

$$\mathrm{M\text{-}M} \underset{k_{-1}}{\overset{\phi_p,\, h\nu}{\rightleftharpoons}} 2\,\mathrm{M} \qquad (1)$$

$$\mathrm{M} + \mathrm{RHal} \xrightarrow{k_2} \mathrm{MHal} + \mathrm{R} \qquad (2)$$

M-M = a metal-metal-bonded dimer, e.g. $Mn_2(CO)_{10}$;
RHal = an alkyl halide; M = a metal radical, e.g. $Mn(CO)_5$

As we show in the Appendix, the overall quantum yield for disappearance of the dimer is given by

$$\phi_t = \frac{2b\phi_p}{(1-T)}\left[\frac{-(\ln 10)b\epsilon CL}{z} + \frac{2}{z}(b^2 - zT)^{1/2} - \frac{2}{z}(b^2 - z)^{1/2} + \frac{b}{z}\ln\left(\frac{(b^2 - zT)^{1/2} - b}{(b^2 - zT)^{1/2} + b}\right) - \frac{b}{z}\ln\left(\frac{(b^2 - z)^{1/2} - b}{(b^2 - z)^{1/2} + b}\right)\right] \qquad (3)$$

where T = transmittance of the solution ($10^{-\epsilon CL}$), ϵ = extinction

* To whom correspondence should be addressed at the Department of Chemistry, University of Oregon, Eugene, OR 97403.

0020-1669/86/1325-0706$01.50/0